# Photo-electrocatalytic hydrogen generation at dye-sensitised electrodes functionalised with a heterogeneous metal catalyst

Dijon A. Hoogeveen[a], Maxime Fournier[a], Shannon A. Bonke[a], Xi-Ya Fang[b], Attila J. Mozer[c], Amaresh Mishra[d,e], Peter Bäuerle[d], Alexandr N. Simonov[a*], Leone Spiccia[a*]

[a] *School of Chemistry and ARC Centre of Excellence for Electromaterials Science, Monash University, Victoria 3800, Australia*; E-mail: alexandr.simonov@monash.edu, leone.spiccia@monash.edu

[b] *Monash Centre for Electron Microscopy, Monash University, Victoria, 3800, Australia*

[c] *Intelligent Polymer Research Institute and ARC Centre of Excellence for Electromaterials Science, University of Wollongong, Wollongong, 2522, Australia*

[d] *Institute for Organic Chemistry II and Advanced Materials, University of Ulm, Albert-Einstein-Allee 11, 89081, Ulm, Germany*

[e] *Current address: School of Chemistry, Sambalpur University, Jyoti Vihar-768019, Sambalpur, India*

**Abstract.** Dye-sensitised photocathodes promoting hydrogen evolution are usually coupled to a catalyst to improve the reaction rate. Herein, we report on the first successful integration of a heterogeneous metal particulate catalyst, *viz.*, Pt aggregates electrodeposited from acidic solutions on the surface of NiO-based photocathode sensitised with a *p*-type perylenemonoimid-sexithiophene-triphenylamine dye (PMI-6T-TPA). The platinised dye-NiO electrodes generate photocurrent density of *ca* -0.03 mA $cm^{-2}$ (geom.) with 100% faradaic efficiency for the $H_2$ evolution at 0.059 V *vs.* reversible hydrogen electrode under 1 sun visible light irradiation (AM1.5G, 100 mW $cm^{-2}$, $\lambda > 400$ nm) for more than 10 hours in 0.1 M $H_2SO_4$ (aq.). The Pt-free dye-NiO and dye-free Pt-modified NiO cathodes show no photo-electrocatalytic hydrogen evolution under these conditions. The performance of these Pt-modified PMI-6T-TPA-based photoelectrodes compares well to that of previously reported dye-sensitised photocathodes for the $H_2$ evolution.

## 1. Introduction

With 120 petawatts of electromagnetic irradiation reaching the surface of the Earth each year, sunlight is the largest sustainable and exploitable energy resource [1,2]. A great challenge exists, however, to take full advantage of this energy through conversion into a storable and transportable fuel [2–6]. Electrochemical water splitting (equation 1) has been widely investigated as a method for 'solar fuel' generation given its use of water as a cheap and abundant feedstock and its production of hydrogen as a carbon free fuel [4,7].

$$2H_2O \rightleftharpoons O_2 + H_2 \qquad \Delta E = 1.23\ \text{V} \qquad (1)$$

$$2H_2O \rightleftharpoons O_2 + 4H^+ + 4e^- \qquad E^0 = 1.23\ \text{V}\ \textit{vs.}\ \text{RHE} \qquad (2)$$

Oxygen Evolution Reaction

$$2H^+ + 2e^- \rightleftharpoons H_2 \qquad E^0 = 0.00\ \text{V}\ \textit{vs.}\ \text{RHE} \qquad (3)$$

Hydrogen Evolution Reaction (HER)

Tandem dye-sensitised (DS) photoelectrochemical cells (PECs) [8] are an emerging photocatalytic water splitting technology built upon foundations laid by research into dye-sensitised solar cells (DSCs) [9]. Both involve the sensitisation of a wide band-gap semiconductor with light harvesting dye molecules. Instead of reversible redox couples, materials catalysing water oxidation (photoanode, eq. 2) and hydrogen evolution (photocathode, eq. 3) are introduced to promote dye regeneration. Our pioneering work focussed on photoanodes [10]. Sun and co-workers subsequently reported transient water oxidation photocurrents above 0.5 mA $cm^{-2}$ under 3 suns AM1.5G irradiation [11]. However, the photopotential of such anodes is not sufficient for complete water splitting and an adjuvant voltage is generally needed, *e.g.* 0.2 V *vs.* reversible hydrogen electrode (RHE) in the study by Sun and co-workers [11]. Alternatively, a photocathode can be introduced in a tandem configuration to give a fully light driven device. However, the efficiencies of the best DS photocathodes reported to date are much lower than those achieved thus far by photoanodes.

On this basis, further progress in tandem DS-PEC water splitting technology relies on the development of photocathodes with much higher activity, and, equally importantly, long-term stability [12].

Till now, there has been few reports on DS photocathodes which satisfactorily promote hydrogen evolution in aqueous medium [13–18]. They all consist of a mesoporous *p*-type NiO layer sensitised with a Ru(II) or organic sensitiser, often functionalised with a molecular HER catalyst. The latter is needed to improve the rate of $H_2$ evolution, which is typically poor on dye surfaces. Promising catalysts include cobalt(II) difluoroboryl-diglyoximate ($CodmgBF_2$) and nickel(II) bis(1,5-R′-diphospha-3,7-R″-diazacyclooctane). These catalysts can be introduced by drop-casting on the DS surface [13], complexing to a co-adsorbed covalent linker [16], direct attachment to the dye [15], or ionic interactions [18]. To our knowledge, there is only one report on coupling a photocathode sensitised with an organic dye to an inorganic catalyst. This was achieved by introducing a molecular $Mo_3S_4$ cluster as a homogeneous HER catalyst into the solution [17]. This successful strategy, imitating to some extent the principle of a *p*-type photocathode in DSCs, resulted in the reductive photocurrent densities of *ca* -150 μA $cm^{-2}$. This performance was achieved over 16 hours continuous illumination (3.44 suns) and conditions favourable for hydrogen evolution, *viz.* in 1.0 M HCl at 0.0 V *vs*. RHE.

Notwithstanding the progress achieved, there are concerns over the stability of the HER photocathode systems while in operation, *viz.* rapid photocurrent loss and faradaic efficiencies well below 100% [13,15–18]. For example, molecular hydrogen measurements for the $Mo_3S_4$-based DS system in Ref. [17], undertaken at the negative potential (-0.30 V *vs*. RHE), indicated a faradaic efficiency of *ca* 50 %. This was attributed to the irreversibility of the $Mo^{4+}$ reduction, and evidence for the co-catalyst decomposition was presented [17].

Overall, the molecular HER catalyst is typically the most fragile component of the photocathode system. Indeed, reductive degradation has been found elsewhere in the literature for cobalt and nickel complexes [19–23] with specific evidence provided in the case of cobaloximes [24], as well as with the cubane $Mo_3S_4$ cluster mentioned above [25]. Thus, both the activity and stability of molecular catalysts coupled so far with DS photocathodes are generally poorer than those of much simpler and, in some cases cheaper, heterogeneous inorganic catalysts, such as Pt-group metals [26] and transition metal sulphides, phosphides or carbides [27]. On top of reasonable activity and robustness, to sustain efficient electron transfer, it is desirable for the catalyst to be in intimate contact with the photoactive sites, as explicitly demonstrated in studies on water-splitting photoanodes [28–30]. However, achieving a favourable alignment of a purely inorganic catalyst on a monolayer of an organic dye is a challenging task. Moreover, the catalyst needs to be well dispersed to achieve optimum performance and efficient utilisation. The latter is very important particularly when using the best known hydrogen evolution electrocatalyst, *viz.* Pt metal [31–33]. Platinum has often been introduced onto non-sensitised narrow band gap photocathodes to promote hydrogen evolution [34–38], but has yet to be integrated to a DS photocathode.

In this study, we report the first successful functionalisation of a dye-sensitised photocathode with platinum particles that function as catalysts for the hydrogen evolution reaction. A *p*-type dye perylenemonoimid-sexithiophene-triphenylamine (PMI-6T-TPA) employed herein has been highly successful for application at *p*-type DSCs [39–42], and even more importantly, has been reported to be capable of sustaining low levels of the light-driven HER without a catalyst [14]. The device assembly and dye structure are shown in Scheme 1.

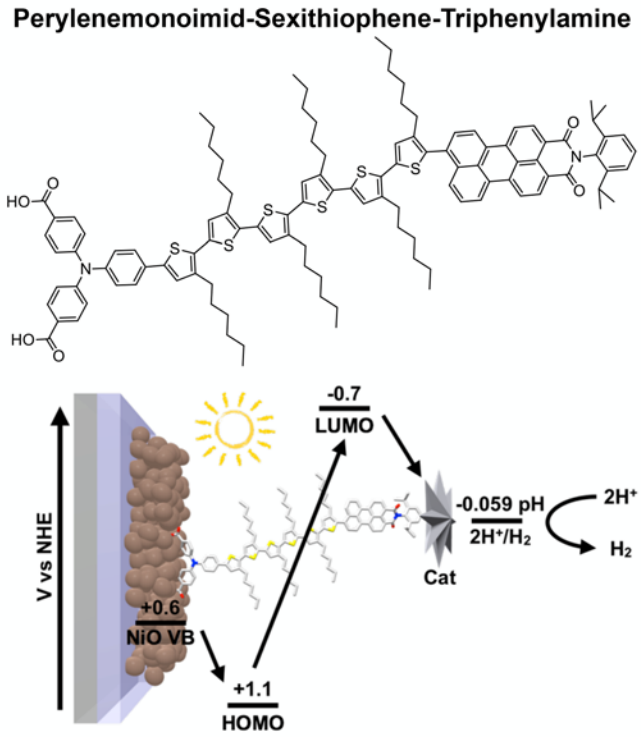


**Scheme 1.** Perylenemonoimid-sexithiophene-triphenylamine dye and schematic energy diagram of the catalyst/dye-NiO photocathode assembly. VB is the NiO valence band. HOMO and LUMO are the highest occupied and lowest unoccupied molecular orbitals of the dye. Cat is the HER catalyst.

## 2. Experimental

### *2.1. Materials*

Reagent or analytical grade chemicals were used as received from commercial suppliers. Reverse osmosis purified water with a quoted resistivity of 1 MΩ cm at 25°C was used in all experimental procedures and to prepare electrolyte solutions unless otherwise stated. Glass coated with fluorine-doped $SnO_2$ (FTO) (sheet resistance *ca.* 8 Ω $sq^{-1}$) was purchased from *Dyesol*. NiO nanoparticle powder (particle size ~20 nm; 73.22 wt.% Ni) was used as received from *Inframat*. The perylenemonoimid-sexithiophene-triphenylamine dye was synthesised following a published procedure [43].

*2.2. Photocathode preparation*

Procedures for the deposition of the NiO layer and its sensitisation with the PMI-6T-TPA dye were adopted from the literature [42,44]. A NiO paste was prepared by mixing NiO, ethyl cellulose solution (5 wt.% in ethanol) and terpineol in the ratio 4 : 23 : 23 (wt.) and ball milling this mixture at 400 rpm for 4 hours (Fritsch Pulverisette 7; 50 ml zirconia cylinder; zirconia balls of 11, 7, 5 and 3 mm diameter). A commercial semi-automatic screen-printer (*Keywell*) was used to print circular NiO films with a geometric area of 2 $cm^2$ on FTO. All current densities reported below are normalised to this area. Two successive printing cycles were performed resulting in a NiO film thickness of *ca.* 1.5 μm as measured using a Veeco Dektak 6M stylus profilometer. The electrodes were sintered at 450°C for 30 min and at 500°C for 15 min on air. Prior to sensitisation, the NiO films were re-sintered at 450°C for 30 min in air, immersed while warm (*ca*. 60°C) into a N,N-dimethylformamide (DMF) solution containing 0.20 mM PMI-6T-TPA and left overnight (15-20 h) at ambient temperature (*ca.* 24°C). The films were then suspended in DMF for 10 mins to remove any uncoupled dye and air dried. Electrical contact was provided by soldering an aluminium wire onto the NiO-free part of the electrode. The uncovered FTO surface was masked using a neutral (non-corrosive) cure silicone sealant (*Selleys*). A photograph of a typical dye-NiO photocathode is shown in Fig. S1 (Supporting Information). For some of the electrodes, 50 μL of a Nafion® perfluorinated resin solution was drop-cast onto the electrode surface and dried to achieve immobilisation to the surface. The Nafion solution was prepared by mixing 50 μL of 5 wt% Nafion (in water and lower aliphatic alcohols) with 750 μL water and 250 μL isopropanol. Prior to testing, wetting of the photocathodes was carried out in an isopropanol : water solution (1 : 1 vol.) followed by thorough rinsing with water.

*2.3. Photo-electrochemical methods*

All electrochemical experiments were performed with a Bio-Logic VSP potentiostat using a three electrode setup under a high-purity Ar atmosphere (99.999%; $O_2 \leq 2$ ppm) unless otherwise specified. A Ag|AgCl|KCl(sat.) reference electrode (*CHI*) was used throughout, but the potentials are reported *versus* RHE according to relationship $E$ vs. RHE = $E$ vs. Ag|AgCl|KCl(sat.) + 0.197 + 0.059pH. A custom made photo-electrochemical cell (PEEK and Teflon body) with a quartz window was used to test the photocathodes with a platinum wire counter electrode confined in a glass-frit separated compartment.

A solar simulator (*Newport*, Model 67005) equipped with a 150 W Xenon lamp with a spectral distribution of AM1.5G and intensity of 1 sun (100 mW $cm^{-2}$) was used as irradiation source. Calibration was achieved by placing a reference solar cell (*CalLab*, Frauenhofer ISE; serial No. 010-2010, calibration mark: 1010-2010014ISE0311) in the light beam and adjusting neutral density filters to reach the stated current-voltage profile and efficiency. Subsequently, a 400 nm band pass filter was positioned to provide only visible light irradiation in the experiments, which was needed to prevent direct band gap excitation of NiO [45,46]. All photo-electrochemical data were obtained by irradiating the working electrodes from the back side (dye- and NiO-free) to avoid sacrificial absorption and/or scattering by the catalyst and $H_2$. Some electrodes were additionally tested under irradiation from the front but the resulting photo-current densities were never higher than those measured with back-side illumination.

*2.4. Measurement of hydrogen evolution*

The $H_2$ evolved during chronoamperometric experiments was analysed with a Perkin-Elmer Clarus 580 gas chromatograph (GC) equipped with a molecular sieve 13X column 45-60 mesh (0.6 m, 1/8 inch, 2.0 mm) thermostated at 30°C and a TCD detector (100°C). The GC analysis was arranged in a continuous flow mode, where a stable and precisely controlled stream of Ar carrier gas (1.0 ml $min^{-1}$; mass-flow controller Bronkhorst EL Flow Select) flushed the gas-

tight photoelectrochemical cell and then filled an injection loop (100 μL) in the chromatograph. The gas mixture in the injection loop was fed at specified intervals into the GC column where the concentration of $H_2$ in the sample was measured. Calibration of the setup was performed using galvanostatic hydrogen evolution from a small area platinum working electrode and a 0.1 M $H_2SO_4$ aqueous electrolyte solution (Fig. S2). Under these conditions, the faradaic yield was assumed to be 100%. The $H_2$ concentration detected in the gas outlet flow was related to the (photo)current density to give the faradaic efficiency of the HER over time. This relationship involves two delays and these are discussed in supporting information.

*2.5. Scanning electron microscopy*

Scanning electron micrographs were recorded on a FEI Magellan 400 XHR FEGSEM instrument with the use of a through lens secondary electron detector and concentric backscatter detector. Energy dispersive X-ray (EDX) point analysis was carried under SEM conditions using a Bruker EDS detector under 10 kV and probe current 0.8 nA. Samples for analysis were cut to size and firmly glued to a SEM stub, and electrical contact was provided to the film surface by a copper tape.

*2.6. Inductively Coupled Plasma-Mass Spectroscopy*

Quantification of transition metal impurities in electrolyte solutions was carried out using a time of flight ICP-MS (*GBC*, Optimass 9500). Solutions were made up in 2 vol.% $HNO_3$ in water from an aliquot of electrolyte solution and spiked with Rh cations as an internal standard to monitor instrumental drift and make linear corrections. Raw analyte counts were standardised by means of a calibration curve constructed through systematic dilutions of commercially available stock solutions, with all dilutions based on mass. Background (baseline) counts were based on $HNO_3$ (2 vol.%) and were subtracted from all measurements.

Analysis of each sample was repeated five consecutive times to ensure high accuracy and reproducibility.

## 3. Results and Discussion

A schematic outline of the dye-sensitised photocathode with associated energetics is illustrated in Scheme 1. Visible light illumination results in the excitation of the PMI-6T-TPA sensitiser followed by its reduction by an electron in the NiO valence band (+0.6 V *vs.* normal hydrogen electrode, NHE) to the now unfilled orbital (+1.1 V *vs.* NHE). The redox potential of the reduced sensitiser (-0.7 V *vs.* NHE) is thermodynamically sufficient for hydrogen to be produced within the pH range 0-11 (-0.059pH V *vs.* NHE). In general, however, organic dyes, such as the PMI-6T-TPA sensitiser, do not efficiently catalyse the two-electron two-proton process in equation 3. Therefore, a catalyst needs to be introduced to facilitate accumulation of the photo-generated electrons and promote H-H bond formation.

### *3.1. Photo-electrocatalytic properties of PMI-6T-TPA-sensitised NiO*

The PMI-6T-TPA dye has been previously reported to sustain the photo-electrochemical hydrogen generation even without a catalyst being present [14], although low current densities were achieved. Importantly, Mozer *et al.* [14] have also demonstrated an impressive long-term stability of the PMI-6T-TPA-sensitised NiO photocathodes (hereinafter, dye-NiO) in aqueous 1.0 M HCl and 1.0 M NaOH. These findings stimulated us to first explore the photo-electrocatalytic properties of the unmodified dye-NiO electrodes.

Electrochemical and photo-electrochemical characterisations were undertaken in aqueous solutions with a neutral pH = 7.0 (1.0 M phosphate buffer) and also in 0.1 M $H_2SO_4$ with pH = 1.0. It is well-established that the HER kinetics becomes more sluggish with an increase in pH [33,47,48], and we hoped to facilitate the process by using acidic solutions. Moreover, recent analysis suggests that it is highly desirable to develop water splitting cathodes and anodes that

function under either acidic or alkaline conditions, not in near-neutral buffered solutions [49]. It is important to emphasise the importance of wetting the dye-sensitised electrodes (see Experimental) prior to electrochemical experiments in aqueous medium. In the absence of this procedure, an order of magnitude lower current densities, both dark and photo-generated, were measured when compared to those presented below.

The cyclic voltammograms of a dye-NiO electrode exhibit a pronounced and stable response associated with the redox transformations of nickel oxide ($Ni^{2+/3+}$) [46] and no other features were detected at more negative potentials. This is exemplified in Figure 1a for 0.1 M $H_2SO_4$ and also in Fig. S4 for 1.0 M phosphate buffer (pH 7.0). The cyclic voltammograms are insignificantly influenced by the pH, while the $Ni^{2+/3+}$ peak potential varies in accordance with a Nernstian relationship for a 1-electron 1-proton transfer, consistent with the literature [46]. These observations suggest that some parts of the NiO surface remain accessible to the electrolyte solution, as previously found in DSC research [40,42]. Published voltammetric data for similar dye-NiO electrodes also exhibited a pronounced $Ni^{2+/3+}$ oxidation signal, although this process was poorly reversible [14]. At the same time, the electrodeposition experiments described below demonstrate substantial differences in the properties of unmodified and dye-treated NiO surface.

Notably, our DS electrodes maintained a stable electrochemical response and there was no evidence of dye desorption after continuous voltammetric cycling and, more importantly, during the long-term photo-electrocatalytic experiments (*vide infra*). Comparison of the voltammograms obtained in the dark and under AM1.5G 100 mW $cm^{-2}$ irradiation with $\lambda > 400$ nm (hereinafter, 1 sun visible light) attests to the capacity of the dye-NiO electrodes to generate a reductive photocurrent in aqueous solutions (Figs. 1a and S4). Its magnitude of *ca* 15-20 μA $cm^{-2}$ was very slightly dependent on applied voltages more negative of the NiO features.

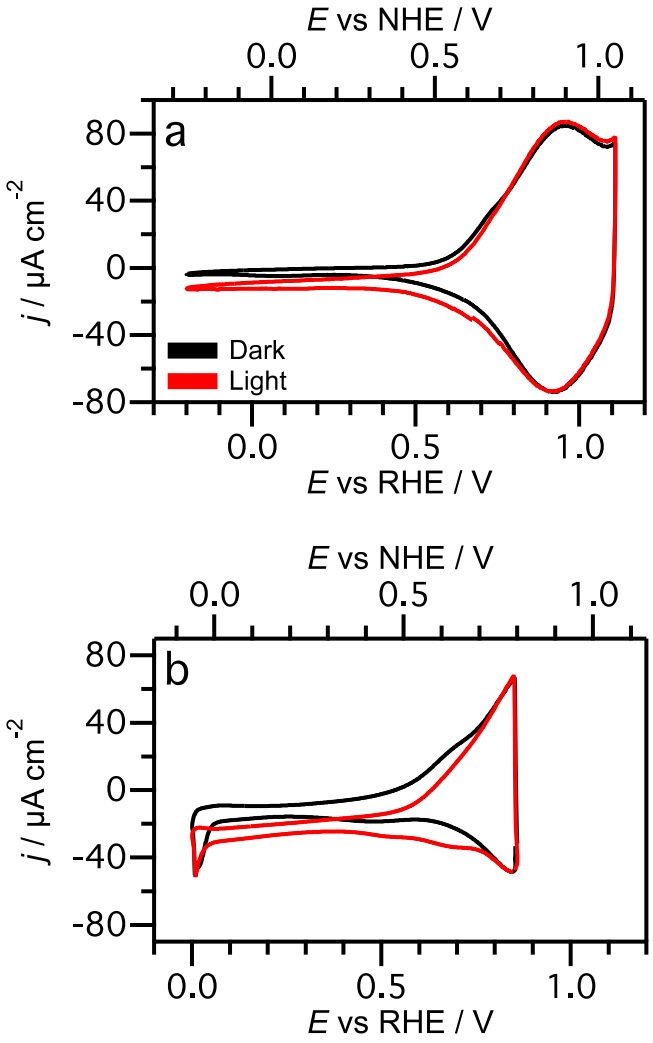


**Figure 1.** Cyclic voltammograms (scan rate, $v$ = 0.010 V $s^{-1}$) of the (a) dye-NiO and (b) $Pt_{ed}$/dye-NiO photocathodes in contact with Ar-saturated 0.1 M $H_2SO_4$ (aq.) in dark (*black*) and under visible light illumination (100 mW $cm^{-2}$, AM 1.5G, λ > 400 nm) (*red*). The second of two scans is shown.

To establish the nature of the reductive current photo-generated by dye-NiO, long-term chronoamperometric experiments were undertaken under illumination at an applied potential of 0.413 V for pH 7.0 (Fig. S5) and 0.059 V for pH = 1.0 (Fig. 2). At both pH values, the reductive photo-current density transients show initial values of about 10 µA $cm^{-2}$ which diminish over the course of two hours to 1-2 µA $cm^{-2}$. To assess the contribution of the HER to the photocurrents, simultaneous $H_2$ detection was undertaken. Considering pH alone, the

sulphuric acid solution should provide more favourable conditions for the electrocatalytic $H_2$ evolution [33,47,48]. Moreover, a more negative potential, on the RHE scale, was used in our experiments at pH = 1.0 as compared to pH = 7.0. In contrast to these expectations, no $H_2$ was produced during more than 10 h long experiments undertaken with dye-NiO in 0.1 M $H_2SO_4$. At the same time, $H_2$ was detected in the presence of phosphate buffer at neutral pH (Figs. 2, S5 and S6), though with a significant delay and at the limits of quantitative detection (Fig. S5). This confirms observations in previous work [14] with major differences in the current densities due to the seven-fold lower intensity of irradiation used herein. Thus, the reductive photo-currents generated by dye-NiO under acidic conditions (Fig. 2) and during initial periods of tests in phosphate buffer (Fig. S5) are mainly due to undesired side reactions, most probably associated with adventitious contaminants in the solution. ICP-MS analysis showed no evidence of metal impurities in the phosphate buffer, but copper at ppb levels was found in 0.1 M $H_2SO_4$ before and after the experiment. We therefore tentatively ascribe the photo-currents measured with dye-NiO in acidic medium to reduction of trace metal impurities and small unavoidable traces of $O_2$. The latter might also produce comparatively high transient reductive photo-current densities in phosphate buffer (Figs. S4 and S5). Indeed, the dye-NiO electrodes are comparatively efficient photo-electrocatalysts for oxygen reduction (Fig. S7).

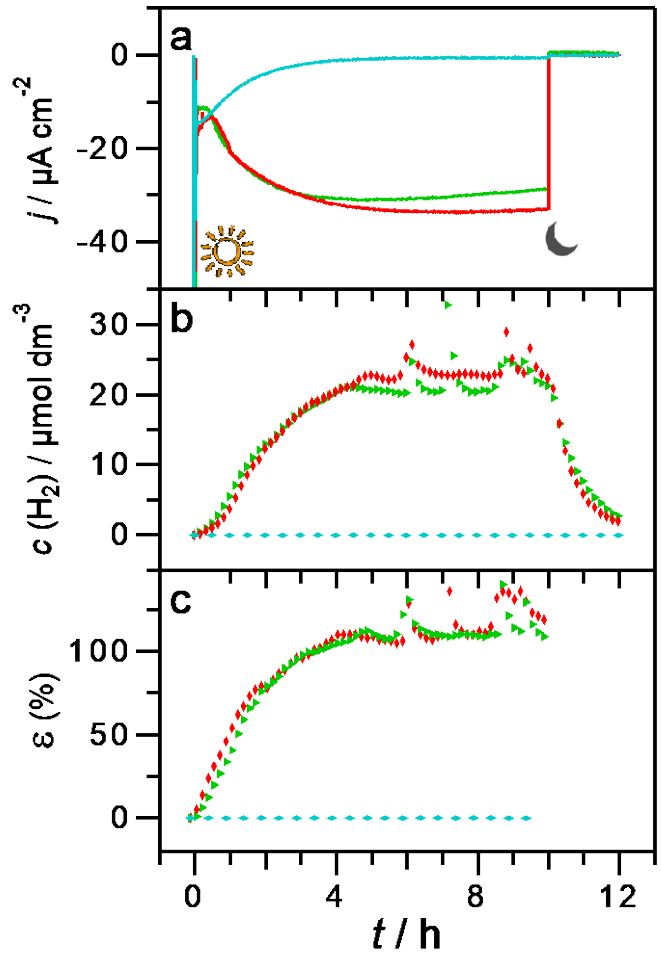


**Figure 2.** (a) Chronoamperometric photo-reduction, (b) $H_2$ concentration in the outlet gas flow and (c) faradaic efficiency for the HER obtained at 0.059 V *vs*. RHE in 0.1 M $H_2SO_4$ under argon using the unmodified dye-NiO (*cyan*), $Pt_{ed}$/dye-NiO (*green*) and $Pt_{ed}$/Nafion/dye-NiO (*red*). Sun and moon pictograms indicate illumination on and off, respectively.

*3.2. Functionalisation of dye-NiO photocathodes with platinum*

Addition of a suitable catalyst to dye-NiO is expected to increase the photo-electrocatalytic hydrogen generation activity of the cathode, which is otherwise unsatisfactory. As mentioned above, nanoparticulate Pt-group metal catalysts have not been surpassed by molecular catalytic systems in terms of both activity and stability during hydrogen evolution, but efficient functionalisation of an organic dye adsorbed on a semiconductor with Pt particles (or other catalysts for that matter) is a non-trivial task. Herein, we have employed a conventional

electrodeposition technique as a first step towards establishing strategies for the successful integration of a heterogeneous catalyst into a dye-sensitised photocathode capable of achieving efficient light-driven $H_2$ evolution.

Reductive electrodeposition from chloroplatinate solutions provides a facile method to immobilise platinum on electro-active surfaces [50–52]. Reduction of $[Pt^{IV}Cl_6]^{2-}$ to $[Pt^{II}Cl_4]^{2-}$ and the latter to $Pt^0$ metal is possible at very positive potentials [53]. However, cyclic voltammograms obtained for the dye-NiO electrodes in a 5 mM $H_2PtCl_6$ + 0.1 M $H_2SO_4$ solution show negligible reductive current densities until the potential reaches *ca* 0.25 V (Fig. 3a). Irradiation of the electrode generates appreciable reductive photocurrents (*cf. red* and *black* data in Fig. 3a), although it seems unlikely that this reduction produces deposits of Pt catalyst capable of accepting electrons from the dye. Indeed, the current remains essentially constant over a wide potential range, when a progressive enhancement, due to the photo-electrocatalytic HER and (photo)electrochemical deposition of Pt would be expected for an electrode where there is efficient charge transfer between PMI-6T-TPA and the catalyst. Some enhancement in the reductive current is observed upon cycling the potential below 0.25 V, which most probably results from an interplay of the $Pt^{IV}Cl_6^{2-}/Pt^{II}Cl_4^{2-}$ reduction and Pt(0) deposition. Fast electrocatalytic hydrogen evolution at potentials more negative than -0.05 V and its reoxidation upon reversing the potential sweep (oxidation peak at *ca* 0.05 V) are indicative of successful Pt deposition on the electrode surface. Yet, the data in Fig. 3 neither confirms nor disproves that the Pt deposit is capable of harvesting photo-generated electrons from the dye. Overall, voltammetric analysis demonstrates that electroreduction of dissolved Pt precursors on the dye-NiO surface is kinetically unfavourable.

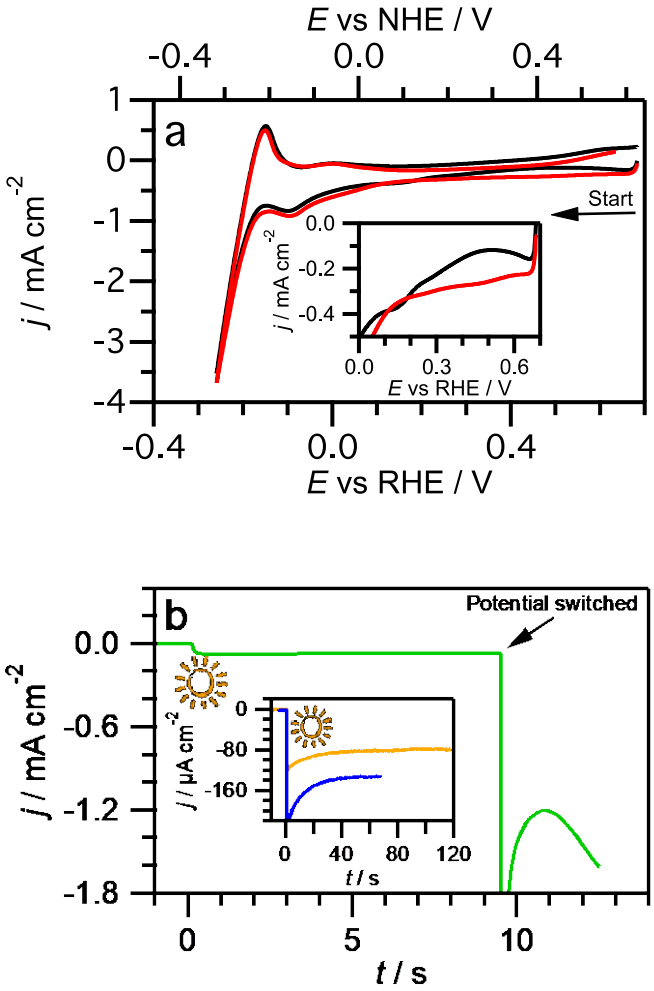


**Figure 3.** Reduction of Ar-saturated 5 mM $H_2PtCl_6$ + 0.1 M $H_2SO_4$ solution using dye-NiO photocathodes. (a) Cyclic voltammetry ($v$ = 0.050 V $s^{-1}$) in the dark (1st cycle) (*black*) and under 1 sun visible light irradiation (2nd cycle) (*red*). (b) Chronoamperometry at 0.76 V ($t$ < 10 s) and -0.14 V *vs.* RHE ($t \geq 10$ s) with irradiation commencing at $t$ = 0 s for unmodified dye-NiO. Inset in panel (a) shows a magnified plot of the initial section of voltammogram. Inset in panel (b) shows current transient at 0.76 V *vs.* RHE with irradiation commencing at $t$ = 0 s for unmodified dye-NiO (*orange*) and $Pt_{ed}$/dye-NiO (*blue*).

Deposition of Pt on the dye-NiO surface was attempted using two further potentiostatic approaches. Control samples were obtained by holding the potential at the open circuit value measured in the dark (*ca.* 0.76 V) and irradiating the electrode until 10 mC $cm^{-2}$ reductive charge is passed (inset to Fig. 3b, *orange*). This was done to assess the capacity of dye-NiO to

photo-reduce $PtCl_6^{2-}$ to Pt metal without application of adjuvant voltage. These samples are referred to as $Pt_{hv}$/dye-NiO. Another type of Pt-modified photocathodes was obtained under conditions known to guarantee Pt(0) deposition (Fig. 3a) by simultaneously applying a potential of -0.14 V and irradiating dye-NiO (Fig. 3b, *green*) for 3 seconds. The corresponding electrodes are referred to as $Pt_{ed}$/dye-NiO. It is noted that similar platinum deposition experiments on dye-free NiO electrodes produced much higher reductive current densities during the first second at -0.14 V and quickly achieved a mass-transport controlled maximum of *ca* 7 mA $cm^{-2}$. This difference in the electrodeposition/HER kinetics on dyed and dye-free electrodes provides further evidence of poor accessibility of the unmodified NiO surface to the electrolyte solution after adsorption of PMI-6T-TPA. Some $Pt_{ed}$/dye-NiO electrodes were also used to deposit more Pt(0) by utilising the photo-reductive potential of dye-NiO to give $Pt_{ed+hv}$/dye-NiO. As for $Pt_{hv}$/dye-NiO, this involved irradiation of the Pt-modified photocathodes while immersed in $PtCl_6^{2-}$ solution and held at open circuit potential measured in the dark (inset to Fig. 3b, *blue*). Notably, the preceding Pt deposition step reduced the time needed for 10 mC $cm^{-2}$ to pass (*cf. orange* and *blue* in Fig. 3b), demonstrating an increased photo-reductive capability of the platinised photocathode.

The cyclic voltammograms of $Pt_{ed}$/dye-NiO in 0.1 M $H_2SO_4$ under argon exhibit features attributable to Pt(0), which are, however, obscured by the background response from dye-NiO (Fig. 1b). Specifically, platinisation of the photocathode induces enhancements in voltammetric currents in the potential region 0.0-0.2 V, where peaks associated with the hydrogen underpotential deposition ($H_{upd}$) on the Pt surface are expected. The poorly defined shape of the $H_{upd}$ peaks is not uncommon at low loadings of electrodeposited Pt [51]. Although the electroactive Pt surface area cannot be determined precisely from voltammetric data, such as those in Fig. 2, an upper limit of 0.06 $cm_{Pt}^2$ $cm_{geom.}^{-2}$ can be estimated for $Pt_{ed}$/dye-NiO by using the background-corrected oxidative $H_{upd}$ charge and the conversion coefficient of 0.21

mC $cm^{-2}$ [54]. Given the exceptionally high electrocatalytic activity of Pt, even this low surface area should be sufficient to maintain reasonable hydrogen evolution rates.

Scanning electron microscopy in the secondary electron (SE) and back-scattered electron (BSE) imaging modes was used to study the morphology of some dye-NiO electrodes after Pt deposition. Since Pt atoms with a higher atomic number scatter electrons more strongly than Ni atoms, BSE imaging allows the identification of Pt rich areas. Fig. 4 shows the SEM analysis of one $Pt_{ed}$/dye-NiO electrode after long-term a photo-electrochemical experiment similar to those shown in Fig. 2. SE imaging reveals the macroporous morphology of the multicomponent photocathode (Fig. 4a,c), while the high contrast BSE micrograph clearly identifies bright Pt particles distributed across the entire sample surface (Fig. 4b). The presence of large aggregates and smaller deposits of Pt was confirmed by point energy dispersive X-ray (EDX) elemental analysis (Fig. 4c) and by Pt elemental mapping (Fig. 4d).

Thus, both electrochemical and SEM/EDX analyses confirm presence of Pt on the dye-NiO surface when electrodeposition is carried out a very high overpotentials for the $Pt^{IV/II/0}$ reduction. However, this does not guarantee that the deposited platinum particles can utilise electrons photo-generated by the underlying PMI-6T-TPA dye. Photo-electrocatalytic tests with simultaneous detection of $H_2$ were subsequently undertaken to establish hydrogen evolution by the photocathode.

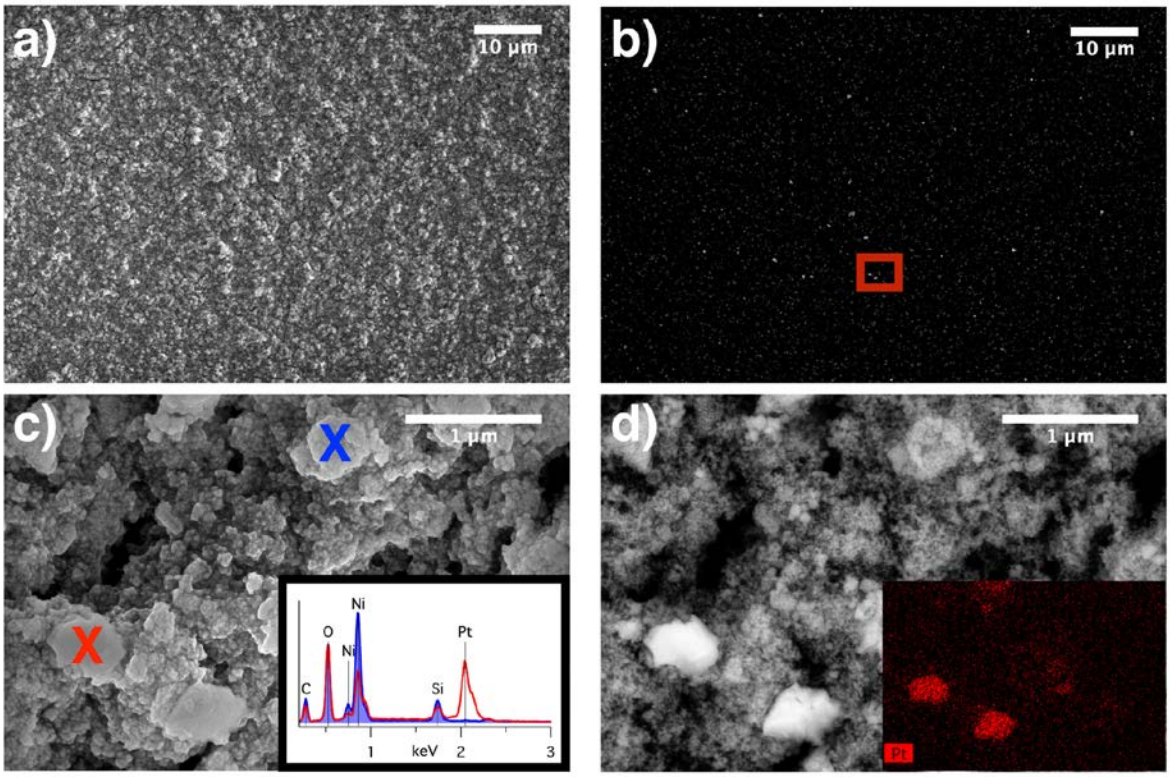


**Figure 4.** SEM characterisation of the $Pt_{ed}$/dye-NiO photocathode after photo-electrocatalytic measurements using (a,c) SE and (b,d) BSE imaging modes. The micrographs in panels (c) and (d) were taken from the area marked with a red box in panel (b), while the inset to panel (d) shows Pt elemental mapping of this area. Inset to panel (c) shows EDX spectra taken from points marked with red and blue crosses.

*3.3. Photo-electrocatalytic hydrogen evolution activity of Pt-functionalised dye-NiO*

The performance of the photocathodes modified with a Pt catalyst was examined in 0.1 M $H_2SO_4$ solutions under argon, which is a favourable environment for hydrogen evolution from noble metal surfaces [33,47,48]. Measurements on the $Pt_{h\nu}$/dyeT-NiO photocathodes and the parent Pt-free electrodes under these conditions showed no detectable $H_2$ generation (data not shown). Notably, little deposition of Pt occurred near the dye photo-active sites under irradiation. Despite the suitable thermodynamic matching of potentials, $PtCl_6^{2-}/Pt^0$ reduction appears to be unfavourable on the dyed surface in the absence of an applied negative potential.

The photo-generated reductive current densities observed during photo-modification with Pt (inset to Fig. 3b) could be assigned to the more facile two-electron $PtCl_6^{2-}/PtCl_4^{2-}$ reduction. In contrast to $Pt_{hv}$/dye-NiO, the $Pt_{ed}$/dye-NiO photocathodes demonstrated significantly enhanced reductive photocurrent densities and, most importantly, steady hydrogen generation during 12 h measurements (Fig. 2). Further attempts to deposit platinum on $Pt_{ed}$/dye-NiO by utilising the photo-reductive ability of the dye did not result in any improvements, *i.e.* $Pt_{ed+hv}$/dye-NiO did not show enhanced activity and stability.

Interestingly, the photo-reductive currents were reproducibly enhanced during the initial several hours of the chronoamperometric experiments with $Pt_{ed}$/dye-NiO, reaching reasonably stable level of *ca* 30 μA $cm^{-2}$ (Fig. 3a). No additional elements were identified on the electrode surface using EDX analysis (Fig. 4), excluding the deposition of adventitious metals present in the $H_2SO_4$ solution as the origin of the photo-current enhancement, and no improvements in activity were observed under the same conditions for a Pt-free electrode (Fig. 2). Most importantly, the increase in photo-current density is matched by a corresponding rise in $H_2$ generation after the first four hours. Fluctuations observed during this period are due to the release of gas bubbles built up on the electrode surface into the headspace. Faradaic efficiency calculations demonstrate values near 100% once headspace equilibrium has been reached. Such a high faradaic efficiency is unprecedented for dye-sensitised photocathodes operating at current densities greater than 5 μA $cm^{-2}$ [15–18].

Despite the reasonable stability of the functioning $Pt_{ed}$/dye-NiO electrode in 0.1 M $H_2SO_4$, a small decrease in photo-current densities was observed after *ca* 7-8 hours of measurements (Fig. 2). To counter this, we have explored the effect of pre-modification of the dye-NiO surface with a perfluorosulfonate ionomer, Nafion®, on the performance and stability of the photocathode. Historically, incorporation of Pt catalyst into Nafion® has been much discussed

as a method to stabilise the activity of noble-metal particles [55,56]. Moreover, similar ionomers are known to improve the efficiency of hydrogen evolution photocathodes comprising a Pt catalyst and a *p*-type Si light-harvester [57]. Nafion® has also been utilised to facilitate incorporation of water oxidation catalysts in the DS photoanodes [10].

The $Pt_{ed}$/Nafion/dye-NiO photocathode was obtained using the electrodeposition protocol employed for the preparation of $Pt_{ed}$/dye-NiO, but using a photocathode pre-modified with a thin layer of Nafion (see Experimental). The reductive photocurrent density for the Nafion-modified and Nafion-free platinised dye-NiO electrodes are similar in magnitude but are more stable for $Pt_{ed}$/Nafion/dye-NiO over the measurement period (Fig. 2). Increases in the measured $H_2$ concentration, without change in the faradaic efficiency, indicate that Nafion results in more stable hydrogen generation.

Given the small electroactive surface area and large size of the catalyst particles in the $Pt_{ed}$-modified dye-NiO electrodes, it is not surprising that comparatively low photo-current densities of the HER were achieved. For such loadings and morphology of Pt, most excited sensitisers will not be in close proximity to the Pt particles to allow for efficient electron transfer. As a result, most photo-generated charge carriers are likely to continue to recombine with holes injected in the NiO, as occurs in the unmodified dye-NiO photocathodes. There is obviously room for optimisation either through substantial improvements in dispersion, increased loading and/or by the introduction of a charge transfer layer that can effectively harvest and transport the charges to the catalyst without substantial potential losses. These studies go beyond the scope of the present study, which exclusively aims to demonstrate the feasibility of coupling a metal hydrogen evolution catalyst with an organic *p*-type sensitiser.

Importantly, the photocathodes developed herein demonstrate reasonable and stable photo-electrocatalytic hydrogen generation with the current density of 30 μA $cm^{-2}$ at 0.059 V *vs*. RHE

at pH = 1.0 under 1 sun visible light irradiation. Moreover, a 100% faradaic efficiency for the HER and outstanding stability of the photo-generated current was achieved resulting in a photoelectrochemical hydrogen evolution rate of 9.1 nmol $cm^{-2}$ $min^{-1}$ $sun^{-1}$. This performance can be compared to 6.6 nmol $cm^{-2}$ $min^{-1}$ $sun^{-1}$ derived from 150 μA $cm^{-2}$ at 0.0 V *vs*. RHE at pH = 0.0 with assumed *ca* 50% faradaic efficiency under *ca* 3.5 sun illumination with the dye coupled to a molecular $Mo_3S_4$ catalyst [17]. Under much less favourable conditions of 0.413 V *vs*. RHE at pH = 7.0, 100 mW $cm^{-2}$ illumination (white LED, $T$ = 6000-6500 K, >400 nm), Sun and co-workers [16] achieved an impressive quasi-stable performance of 4.1 nmol $cm^{-2}$ $min^{-1}$ $sun^{-1}$ that corresponds to 20 μA $cm^{-2}$ after 90 min with *ca* 68% faradaic efficiency using a co-adsorbed cobaloxime catalyst (assuming that the irradiation source matches the AM1.5G spectrum). On balance, the performance achieved by our Pt-modified dye-NiO electrodes is similar to that of the best HER photocathodes reported so far (see Refs. [16,17]).

## 4. Conclusions

In summary, we have demonstrated that platinum particles can be deposited onto the PMI-6T-TPA dye-sensitised NiO photocathode and can utilise photo-generated electrons to catalyse hydrogen evolution in acidic medium. Modification of dye-NiO with Pt metal is achieved *via* facile electrodeposition process. SEM/EDX characterisation shows low loadings of comparatively large Pt particles spread over the electrode surface pointing to further opportunities for improvement. Most importantly, the photocathode operates efficiently under acidic conditions, which are favourable for the HER. Hydrogen generation photocurrents of 30 μA $cm^{-2}$ and a faradaic efficiency of 100% are demonstrated at +0.059 V *vs.* RHE under 1 sun irradiation over 10 hours, which match the performance of the state-of-the-art dye-sensitised photocathodes. Improvements in the stability of the photocathode have been possible *via* coating the dye surface with solid electrolyte Nafion®.

The results reported herein demonstrate that integration of a heterogeneous catalyst with an organic dye affords a robust photocathodes that can selectively generate hydrogen in strongly acidic medium. We believe that the success of the devised strategy and obvious room for improvements will lead to photocathodes capable of matching the performance of their photoanode counterparts allowing the development of efficient and robust tandem DS-PEC water-splitting devices.

**Acknowledgements**

The authors acknowledge the Australian Research Council for providing financial support for this study through the ARC Centre of Excellence for Electromaterials Science (Grant No. CE140100012), the School of Chemistry (Monash University) for providing research facilities to carry out this work, the Monash Centre for Electron Microscopy (Monash University) for providing microscopy facilities.

**References**

[1] N. Armaroli, V. Balzani, The future of energy supply: Challenges and opportunities, Angew. Chem. Int. Ed. 46 (2007) 52–66. doi:10.1002/anie.200602373.

[2] N.S. Lewis, D.G. Nocera, Powering the planet: Chemical challenges in solar energy utilization, Proc. Natl. Acad. Sci. 103 (2006) 15729–15735. doi:10.1073/pnas.0603395103.

[3] T.A. Faunce, W. Lubitz, A.W. Rutherford, D. MacFarlane, G.F. Moore, P. Yang, D.G. Nocera, T.A. Moore, D.H. Gregory, S. Fukuzumi, K.B. Yoon, F.A. Armstrong, M.R. Wasielewski, S. Styring, Energy and environment policy case for a global project on artificial photosynthesis, Energy Environ. Sci. 6 (2013). doi:10.1039/c3ee00063j.

[4] A.J. Bard, M.A. Fox, Artificial photosynthesis: Solar splitting of water to hydrogen and oxygen water splitting, Acc. Chem. Res. 28 (1995) 141–145.

doi:10.1021/ar00051a007.

[5] S. Styring, Artificial photosynthesis for solar fuels, J. Chem. Soc. Faraday Trans. 155 (2012) 357–376. doi:10.1038/nphoton.2012.175.

[6] S. Dahl, I. Chorkendorff, Solar-fuel generation: Towards practical implementation, Nat. Mater. 11 (2012) 100–101. doi:10.1038/nmat3233.

[7] B.D. Sherman, M.D. Vaughn, J.J. Bergkamp, D. Gust, A.L. Moore, T.A. Moore, Evolution of reaction center mimics to systems capable of generating solar fuel, Photosynth. Res. 120 (2014) 59–70. doi:10.1007/s11120-013-9795-4.

[8] W. Song, Z. Chen, C.R.K. Glasson, K. Hanson, H. Luo, M.R. Norris, D.L. Ashford, J.J. Concepcion, M.K. Brennaman, T.J. Meyer, Interfacial dynamics and solar fuel formation in dye-sensitized photoelectrosynthesis cells, ChemPhysChem. 13 (2012) 2882–2890. doi:10.1002/cphc.201200100.

[9] W.J. Youngblood, S.-H.A. Lee, K. Maeda, T.E. Mallouk, Visible light water splitting using dye-sensitized oxide semiconductors., Acc. Chem. Res. 42 (2009) 1966–1973. doi:10.1021/ar9002398.

[10] R. Brimblecombe, A. Koo, G.C. Dismukes, G.F. Swiegers, L. Spiccia, Solar driven water oxidation by a bioinspired manganese molecular catalyst, J. Am. Chem. Soc. 132 (2010) 2892–2894. doi:10.1021/ja910055a.

[11] Y. Gao, X. Ding, J. Liu, L. Wang, Z. Lu, L. Li, L. Sun, Visible light driven water splitting in a molecular device with unprecedentedly high photocurrent density, J. Am. Chem. Soc. 135 (2013) 4219–4222. doi:10.1021/ja400402d.

[12] Z. Yu, F. Li, L. Sun, Recent advances in dye-sensitized photoelectrochemical cells for solar hydrogen production based on molecular components, Energy Environ. Sci. 8 (2015) 760–775. doi:10.1039/c4ee03565h.

[13] L. Li, L. Duan, F. Wen, C. Li, M. Wang, A. Hagfeldt, L. Sun, Visible light driven

hydrogen production from a photo-active cathode based on a molecular catalyst and organic dye-sensitized p-type nanostructured NiO, Chem. Commun. 48 (2012) 988–990. doi:10.1039/c2cc16101j.

[14] L. Tong, A. Iwase, A. Nattestad, U. Bach, M. Weidelener, G. Götz, A. Mishra, P. Bäuerle, R. Amal, G.G. Wallace, A.J. Mozer, Sustained solar hydrogen generation using a dye-sensitised NiO photocathode/BiVO4 tandem photo-electrochemical device, Energy Environ. Sci. 5 (2012) 9472–9475. doi:10.1039/c2ee22866a.

[15] Z. Ji, M. He, Z. Huang, U. Ozkan, Y. Wu, Photostable p-type dye-sensitized photoelectrochemical cells for water reduction, J. Am. Chem. Soc. 135 (2013) 11696–11699.

[16] F. Li, K. Fan, B. Xu, E. Gabrielsson, Q. Daniel, L. Li, L. Sun, Organic dye-sensitized tandem photoelectrochemical cell for light driven water splitting, J. Am. Chem. Soc. 137 (2015) 9153–9159. doi:10.1021/jacs.5b04856.

[17] K.A. Click, D.R. Beauchamp, Z. Huang, W. Chen, Y. Wu, Membrane-Inspired Acidically Stable Dye-Sensitized Photocathode for Solar Fuel Production, J. Am. Chem. Soc. 138 (2016) 1174–1179. doi:10.1021/jacs.5b07723.

[18] M.A. Gross, C.E. Creissen, K.L. Orchard, E. Reisner, Photoelectrochemical hydrogen production in water using a layer-by-layer assembly of a Ru dye and Ni catalyst on NiO, Chem. Sci. 07 (2016) 5537. doi:10.1039/C6SC00715E.

[19] S. El Ghachtouli, R. Guillot, F. Brisset, A. Aukauloo, Cobalt-based particles formed upon electrocatalytic hydrogen production by a cobalt pyridine oxime complex, ChemSusChem. 6 (2013) 2226–2230. doi:10.1002/cssc.201300564.

[20] S. Cherdo, S. El Ghachtouli, M. Sircoglou, F. Brisset, M. Orio, A. Aukauloo, A nickel dimethyl glyoximato complex to form nickel based nanoparticles for electrocatalytic H 2 production, Chem. Commun. 50 (2014) 13514–13516. doi:10.1039/c4cc05355a.

[21] E. Anxolabéhère-Mallart, C. Costentin, M. Fournier, S. Nowak, M. Robert, J.M. Savéant, Boron-capped tris(glyoximato) cobalt clathrochelate as a precursor for the electrodeposition of nanoparticles catalyzing H 2 evolution in water, J. Am. Chem. Soc. 134 (2012) 6104–6107. doi:10.1021/ja301134e.

[22] L. Chen, G. Chen, C.F. Leung, S.M. Yiu, C.C. Ko, E. Anxolabéhère-Mallart, M. Robert, T.C. Lau, Dual homogeneous and heterogeneous pathways in photo- and electrocatalytic hydrogen evolution with nickel(II) catalysts bearing tetradentate macrocyclic ligands, ACS Catal. 5 (2015) 356–364. doi:10.1021/cs501534h.

[23] N. Kaeffer, A. Morozan, J. Fize, E. Martinez, L. Guetaz, V. Artero, The dark side of molecular catalysis: diimine–dioxime cobalt complexes are not the actual hydrogen evolution electrocatalyst in acidic aqueous solutions, ACS Catal. (2016) 3727–3737. doi:10.1021/acscatal.6b00378.

[24] E. Anxolabéhère-Mallart, C. Costentin, M. Fournier, M. Robert, Cobalt-bisglyoximato diphenyl complex as a precatalyst for electrocatalytic H2 evolution, J. Phys. Chem. C. 118 (2014) 13377–13381. doi:10.1021/jp500813r.

[25] W. Zhang, T. Zhou, J. Zheng, J. Hong, Y. Pan, R. Xu, Water-Soluble MoS3 Nanoparticles for Photocatalytic H2 Evolution, ChemSusChem. 8 (2015) 1464–1471. doi:10.1002/cssc.201500067.

[26] J. Durst, C. Simon, F. Hasche, H. a. Gasteiger, Hydrogen Oxidation and Evolution Reaction Kinetics on Carbon Supported Pt, Ir, Rh, and Pd Electrocatalysts in Acidic Media, J. Electrochem. Soc. 162 (2014) F190–F203. doi:10.1149/2.0981501jes.

[27] P.C.K. Vesborg, B. Seger, I. Chorkendorff, Recent Development in Hydrogen Evolution Reaction Catalysts and Their Practical Implementation, J. Phys. Chem. Lett. 6 (2015) 951–957. doi:10.1021/acs.jpclett.5b00306.

[28] R. Abe, M. Higashi, K. Domen, Facile Fabrication of an Efficient Oxynitride TaON

Photoanode for Overall Water Splitting into H2 and O2 under Visible Light Irradiation, J. Am. Chem. Soc. 132 (2010) 11828–11829.

[29] S. Singh Gujral, A.N. Simonov, X.-Y. Fang, M. Higashi, T. Gengenbach, R. Abe, L. Spiccia, Photo-assisted electrodeposition of manganese oxide on TaON anodes: effect on water photooxidation capacity under visible light irradiation, Catal. Sci. Technol. 6 (2016) 3745–3757. doi:10.1039/C5CY01432H.

[30] S.S. Gujral, A.N. Simonov, M. Higashi, X.-Y. Fang, R. Abe, L. Spiccia, Highly Dispersed Cobalt Oxide on TaON as Efficient Photoanodes for Long-Term Solar Water Splitting, ACS Catal. 6 (2016) 3404–3417. doi:10.1021/acscatal.6b00629.

[31] N.M. Markovic, S.T. Sarraf, H.A. Gasteiger, P.N. Ross, Surfaces in Alkaline Solution, J. Chem. Soc. Faraday Trans. 92 (1996) 3719–3725.

[32] N.M. Marković, B.N. Grgur, P.N. Ross, Temperature-Dependent Hydrogen Electrochemistry on Platinum Low-Index Single-Crystal Surfaces in Acid Solutions, J. Phys. Chem. B. 101 (1997) 5405–5413. doi:10.1021/jp970930d.

[33] W. Sheng, H.A. Gasteiger, Y. Shao-Horn, Hydrogen Oxidation and Evolution Reaction Kinetics on Platinum: Acid vs Alkaline Electrolytes, J. Electrochem. Soc. 157 (2010) B1529. doi:10.1149/1.3483106.

[34] O. Khaselev, J.A. Turner, A Monolithic Photovoltaic-Photoelectrochemical Device for Hydrogen Production via Water Splitting, Science (80-. ). 280 (1998) 425–427. doi:10.1126/science.280.5362.425.

[35] E. Aharon-Shalom, A. Heller, Efficient p-lnP ( Rh-H alloy ) and p-lnP ( Re-H alloy ) Hydrogen Evolving Photocathodes, J. Electrochem. Soc. 129 (1982) 2865–2866. doi:10.1149/1.2123695.

[36] S.W. Boettcher, E.L. Warren, M.C. Putnam, E.A. Santori, D. Turner-Evans, M.D. Kelzenberg, M.G. Walter, J.R. McKone, B.S. Brunschwig, H.A. Atwater, N.S. Lewis,

Photoelectrochemical hydrogen evolution using Si microwire arrays, J. Am. Chem. Soc. 133 (2011) 1216–1219. doi:10.1021/ja108801m.

[37] B. Seger, T. Pedersen, A. Laursen, P. Vesborg, O. Hansen, I. Chorkendorff, Using TiO2 as a Conductive Protective Layer for Photocathodic H Evolution, J. Am. Chem. Soc. 135 (2013) 1057–1064. doi:10.1021/ja309523t.

[38] J.R. McKone, A.P. Pieterick, H.B. Gray, N.S. Lewis, Hydrogen evolution from Pt/Ru-coated p-type WSe2 photocathodes, J. Am. Chem. Soc. 135 (2013) 223–231. doi:10.1021/ja308581g.

[39] A. Nattestad, A.J. Mozer, M.K.R. Fischer, Y. Cheng, A. Mishra, P. Bäuerle, U. Bach, Highly efficient photocathodes for dye-sensitized tandem solar cells, Nat. Mater. 3 (2010) 31–35. doi:10.1002/cssc.201000042.

[40] S. Powar, T. Daeneke, M.T. Ma, D. Fu, N.W. Duffy, G. Götz, M. Weidelener, A. Mishra, P. Bäuerle, L. Spiccia, U. Bach, Highly efficient p-type dye-sensitized solar cells based on tris(1,2-diaminoethane)cobalt(II)/(III) electrolytes, Angew. Chem. Int. Ed. 52 (2013) 602–605. doi:10.1002/anie.201206219.

[41] T. Daeneke, Z. Yu, G.P. Lee, D. Fu, N.W. Duffy, S. Makuta, Y. Tachibana, L. Spiccia, A. Mishra, P. Bäuerle, U. Bach, Dominating energy losses in NiO p-type dye-sensitized solar cells, Adv. Energy Mater. 5 (2015) 1401387–1401387. doi:10.1002/aenm.201401387.

[42] I.R. Perera, T. Daeneke, S. Makuta, Z. Yu, Y. Tachibana, A. Mishra, P. Bäuerle, C.A. Ohlin, U. Bach, L. Spiccia, Application of the tris(acetylacetonato)iron(III)/(II) redox couple in p-type dye-sensitized solar cells, Angew. Chem. Int. Ed. 54 (2015) 3758–3762. doi:10.1002/anie.201409877.

[43] Q. Wang, S.M. Zakeeruddin, J. Cremer, P. Bäuerle, R. Humphry-Baker, M. Grätzel, Cross surface ambipolar charge percolation in molecular triads on mesoscopic oxide

films, J. Am. Chem. Soc. 127 (2005) 5706–5713. doi:10.1021/ja0426701.

[44] I.R. Perera, A. Gupta, W. Xiang, T. Daeneke, U. Bach, R.A. Evans, C.A. Ohlin, L. Spiccia, Introducing manganese complexes as redox mediators for dye-sensitized solar cells, Phys. Chem. Chem. Phys. 16 (2014) 12021. doi:10.1039/c3cp54894e.

[45] D. Adler, J. Feinleib, Electrical and optical properties of narrow-band materials, Phys. Rev. B. 2 (1970) 3112–3134. doi:10.1103/PhysRevB.2.3112.

[46] G. Boschloo, A. Hagfeldt, Spectroelectrochemistry of nanostructured NiO, J. Phys. Chem. B. 105 (2001) 3039–3044. doi:10.1021/jp003499s.

[47] J. Durst, A. Siebel, C. Simon, F. Hasche, J. Herranz, H.A. Gasteiger, New insights into the electrochemical hydrogen oxidation and evolution reaction mechanism, Energy Environ. Sci. 7 (2014) 2255–2260. doi:10.1039/c4ee00440j.

[48] W. Sheng, Z. Zhuang, M. Gao, J. Zheng, J.G. Chen, Y. Yan, Correlating hydrogen oxidation and evolution activity on platinum at different pH with measured hydrogen binding energy, Nat. Commun. 6 (2015) 5848. doi:10.1038/ncomms6848.

[49] M.R. Singh, K. Papadantonakis, C. Xiang, N.S. Lewis, An electrochemical engineering assessment of the operational conditions and constraints for solar-driven water-splitting systems at near-neutral pH, Energy Environ. Sci. 8 (2015) 2760–2767. doi:10.1039/c5ee01721a.

[50] A.M. Feltham, M. Spiro, Platinized platinum electrodes, Chem. Rev. 71 (1971) 177–193. doi:10.1021/cr60270a002.

[51] A.N. Simonov, O. V. Cherstiouk, S.Y. Vassiliev, V.I. Zaikovskii, A.Y. Filatov, N.A. Rudina, E.R. Savinova, G.A. Tsirlina, Potentiostatic electrodeposition of Pt on GC and on HOPG at low loadings: Analysis of the deposition transients and the structure of Pt deposits, Electrochim. Acta. 150 (2014) 279–289. doi:10.1016/j.electacta.2014.10.098.

[52] A.G. Oshchepkov, A.N. Simonov, P.A. Simonov, A.N. Shmakov, N.A. Rudina, A. V.

Ishchenko, O. V. Cherstiouk, V.N. Parmon, Interrelation between catalytic activity for oxygen electroreduction and structure of supported platinum, J. Electroanal. Chem. 729 (2014) 34–42. doi:10.1016/j.jelechem.2014.07.006.

[53] A.J. Bard, L.R. Faulkner, Electrochemical methods : fundamentals and applications, Wiley, 2001.

[54] S. Trasatti, O.A. Petrii, Real surface area measurements in electrochemistry, J. Electroanal. Chem. 327 (1992) 353–376. doi:10.1016/0022-0728(92)80162-W.

[55] D.R. Lawson, Oxygen reduction at nafion film-coated platinum electrodes: Transport and kinetics, J. Electrochem. Soc. 135 (1988) 2247–2253. doi:10.1149/1.2096247.

[56] Y.M. Maksimov, B.I. Podlovchenko, T.L. Azarchenko, Preparation and electrocatalytic properties of platinum microparticles incorporated into polyvinylpyridine and Nafion films, Electrochim. Acta. 43 (1998) 1053–1059. doi:10.1016/S0013-4686(97)00277-6.

[57] R.N. Dominey, N.S. Lewis, J.A. Bruce, D.C. Bookbinder, M.S. Wrighton, Improvement of photoelectrochemical hydrogen generation by surface modification of p-type silicon semiconductor photocathodes, J. Am. Chem. Soc. 104 (1982) 467–482. doi:10.1021/ja00366a016.